Molecular design targets and optimization of low-temperature thermal desalination systems

Alejandro Garciadiego[a], Tengfei Luo[b], Alexander W. Dowling[a,*]

[a]*Department of Chemical and Biomolecular Engineering*
[b]*Department of Aerospace and Mechanical Engineering*
University of Notre Dame, Notre Dame, IN 46556

Abstract

Access to clean, freshwater is an ever-growing concern for modern society as it is critical to ensure human health, protect threatened ecosystems, and promote economic growth and prosperity. While desalination is a promising pathway to meet global water demands, modern desalination processes remain energy-intensive. Directional solvent extraction (DSE) is an emerging membrane-free liquid-liquid extraction process to desalinate water using low-grade heat. Several unique features make DSE a potentially disruptive desalination technology: 1) it is thermally driven and utilizes low-grade heat; 2) it does not require the use of membranes; 3) there are opportunities to intensify, modularize and customize the process; 4) there is a vast solvent molecular engineering design space. Previous work includes success demonstration of a batch bench-scale DSE process, molecular simulations to understand solvent performance, and heat integration analysis of a single-stage pseudo-steady state DSE process.

In this work, we propose a mathematical modeling framework for simultaneous technoeconomic optimization and heat integration of the DSE process. Using the framework, we perform rapid bottom-up screening to predict the performance of known organic acid and ionic liquid directional solvents in an optimized DSE process. We then use the optimization framework to identify continuous solvent property targets necessary to realize a levelized cost of wa-

---

[*] Corresponding author
Email address: `adowling@nd.edu` (Alexander W. Dowling)

ter (LCOW) of less than \$0.50/m^3. Specifically, we find the thermoresponsive ability of the solvent and solubility of the solvent in water at a reference temperature are the most influential properties over the cost of the DSE process. Fatty acids are unable to achieve the LCOW goal due to the low thermoresponsive ability of the solvent. However, ionic liquids hold promise. Most importantly, we find a need to engineer ionic liquids with a lower solubility in saline reject.

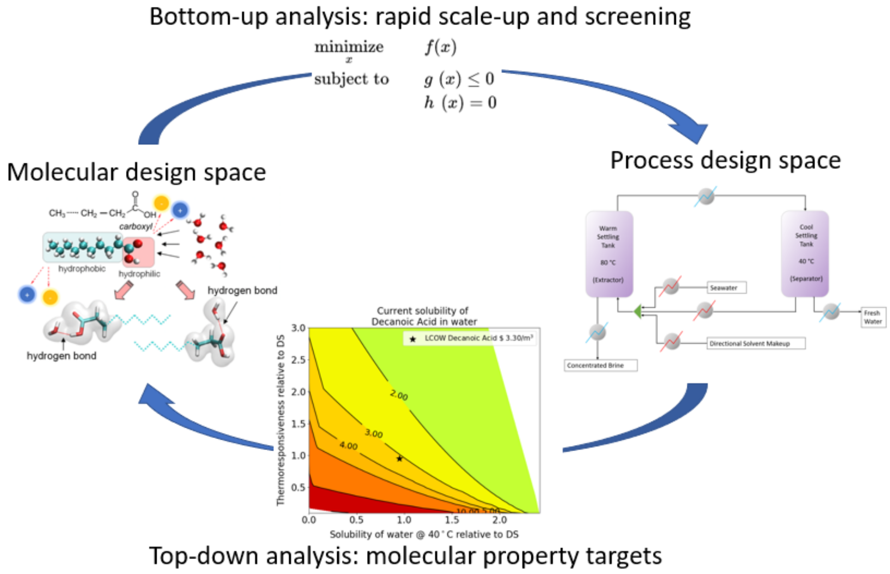

Graphical abstract

Keywords: Desalination, Directional solvent extraction, Process modeling and optimization, Technoeconomic analysis

---

1. Highlights

- DSE is a potentially transformative low-grade heat renewable desalination technology.
- Proposed an optimization framework for DSE and enabled property target search for solvents leading to 10x improvement in LCOW.

- Identified change in solubility of water in the directional solvent with respect to temperature (thermoresponsiveness) and the solubility of the solvent in saline water reject as the most important properties for DSE techno-economic performance.
- Identified a necessary 50 fold reduction of solubility of the solvent in freshwater for solvents with high cost ($100/kg).

2. Introduction

Water consumption is critical to modern society; the average American family uses approximation 1140 liters of municipal water per day [1], and 130 million Americans face severe water scarcity at least part of the year [2]. Globally, 3.8 billion people currently experience water scarcity [3], and it is estimated that 66% of the world's population could be living under water-stressed conditions by 2025 [4]. Although the costs of water obtained from desalination have fallen in the last decade, they are higher than obtaining freshwater from rivers, groundwater, or water recycling. In 2015, less than one percent of the water consumed globally was produced by desalination [5].

The expansion of oil and gas extraction in the US has created new water and environmental challenges [1]. In 2012, 3.57 billion m^3 of produced water was extracted in the US. In the Delaware Basin, up to 4 barrels of water are produced per barrel of oil [6]; to put this number in perspective, around 0.50 liters of produced water may be generated to supply energy for one hour in an average American household. The salinity of produced water is typically 35,000 ppm - 300,000 ppm, which may be up to eight times higher than seawater salinity (35,000 ppm) [7]. Produced water desalination is challenging as current desalination technologies are unpractical to treat high salinity brines [8]. Large water volumes (about 20,000 m^3 on average per well) remain challenging, even after supply chain optimization. [9, 10]. However, in conjunction with water supply chain management innovations, there is a pressing need for new technologies to treat produced water.

Water classification	Salinity (weight%)	Salinity (ppm)	Use	MSF	MED	RO	DSE
Freshwater	0-0.10%	0-1,000 ppm	Human consumption, livestock and irrigation	✓	✓	✓	✓
Slightly saline water	0.10-0.16%	1,000-1,600 ppm	Livestock, may require special treatment for irrigation	✓	✓	✓	✓
	0.16-0.30%	1,600-3,000 ppm	Poultry and pigs	✓	✓	✓	✓
Moderately saline water	0.30-1.00%	3,000-10,000 ppm	Suitable for cattle or sheep and for flushing toilets	✓	✓	✓	✓
Very saline water	1.00-3.50%	10,000-35,000 ppm	Industrial usage(2%), thermoelectric power plants (95%) and mining (3%)	✗	✗	✓(partially)	✓
Briny water	>3.50%	>35,000 ppm		✗	✗	✗	✓

Table 1: Natural and man made sources of water range from freshwater (0-0.10% salinity) to briny water (>3.50% salinity) [1]. Salinity requirements vary widely depending on end use. For example, low salinity water is used for human and livestock consumption. But high salinity water with more than 35,000 ppm is suitable for industrial uses including power plant cooling and mining. While well-established technologies including Multi-stage Flash (MSF), Multi-effect Desalination (MED) and Reverse Osmosis (RO) have greatly advanced desalination industry [11], there remains a need for sustainable and energy efficient process to treat high salinity water. Directional Solvent Extraction (DSE) has been proven to be able to treat high salinity brines while utilizing low-grade heat.

There is no one-size-fits-all technology for water treatment. Instead, there is a growing emphasis on fit-for-purpose treatment in decentralized networks [12]. In this paradigm, water is treated to only the specifications needed for specific end uses. Table 1 highlights different water quality levels (salinity), appropriate end uses, and candidate desalination technologies. While evaporative and reverse osmosis desalination technologies are commonly deployed, they remain energy-intensive and unable to treat high salinity water sources. In the context of fit-for-purpose water, there is a great need for new technologies to treat a wide range of water quality levels in distributed networks while using renewable energy.

Directional solvent extraction (DSE) uses a thermoresponsive solvent to facilitate treatment over a wide salinity range [13]. DSE does not require membranes, which often foul at high salinities, and can utilize low-grade heat, including waste or renewable (solar) sources. Prior work in DSE includes characterization of molecular phenomena, bench-scale demonstrations, and limited process analysis [14, 15, 13, 16, 17, 18]. This paper presents a techno-economic optimization framework with two new capabilities: first, we perform simultaneous process optimization and heat integration to rapidly screen directional solvent candidates in seconds. Second, we perform a sensitivity analysis to identify the necessary solvent properties to enable cost-effective DSE processes for a specific application. We emphasize these advances in process-scale models can rapidly accelerate DSE development by reducing the need for expensive experiments and guiding (computational) molecular design. To our knowledge, this is the first application of equation-oriented process optimization to facilitate bottom-up and top-down analysis of the DSE process.

The remainder of this paper is organized as follows. Section 2 reviews literature on desalination and DSE, with an emphasis on the scope for optimization. Section 3 describes the optimization framework and mathematical models. Section 4 studies the impact of heat source temperature and solvent properties on the optimized process's minimum specific energy. Section 5 presents quantitative solvent property goals to achieve \$0.50/m^3 LCOW target for two classes of molecules: carboxylic acids and ionic liquids. Finally, Section 6 summarizes conclusions, limitations, and future work.

3. Literature review

3.1. Desalinaton technologies

Modern desalination technologies, including evaporative and reverse osmosis systems, are energy-intensive and not suitable to treat high salinity water. Evaporative systems such as multi-stage flash (MSF) and multi-effect distillation (MED) utilize thermal energy (typically 90°C and 55°C, respectively) to evaporate and condensate water [7]. These systems require highly corrosion-resistant and costly materials [19] and are heat-intensive (26.29-83.06 kWh/m^3); they require three or four times the theoretical minimum energy of separation [8, 7]. In contrast, membrane-based technologies such as reverse osmosis (RO) use mechanical work to overcome the osmotic pressure across a membrane. Membrane-based technologies use significant electricity inputs, need frequent membrane replacement, and have limited effectiveness when treating concentrated brines [8]. New technologies, including electrodialysis and forward osmosis, show promise to reduce energy consumption and lower costs. For example, osmotically assisted reverse osmosis (OARO) and mechanical vapor compression (MVC) are suitable to treat high salinity brines (140,000 ppm and 150,000 ppm respectively) [20, 21, 22]. Nevertheless, MVC energy consumption is high (single-effect MVC 2342kWh/m^3, double-effect MVC 20kWh/m^3) [22]. OARO, RO, and other membrane-based technologies are often susceptible to membrane fouling at high salt concentrations [23]. While hybrid desalination systems paired with renewable energy sources are well-studied [24, 25, 26], there is limited work of technologies suitable for high salinity brines.

Table 2: Comparison of energetics, costs, and limitations of common desalination technologies [7, 23].

Technology	Multi-Stage Flash (MSF)	Multi-Effect Distillation (MED)	Reverse Osmosis (RO)
Specific energy	26.29-83.06 kWh/m^3	26.29-76.26 kWh/m^3	3.05-8.33 kWh/m^3
Thermal input temperature	90 °C	55-70 °C	ambient
Global deployment	8%	27%	60%
Cost	0.27-1.49 \$/m^3	0.80-1.50 \$/m^3	0.45-1.62 \$/m^3
Thermal energy input	High	High	Low
Electric energy input	Low	Low	High
Equipment size	Large	Large	Small
Membrane replacement or fouling	No	No	Yes

3.2. Directional Solvent Extraction

Directional solvent extraction can overcome limitations of thermal and membrane-based systems by efficiently separating high salinity feeds with low-grade waste heat (40 - 80 °C). DSE exploits thermoresponsive solvents that extract water from salty mixtures at elevated temperatures and release water (phase separate) when cooled. Directional Solvents (DS) have several features: (1) water can dissolve in the solvent, and the solubility increases with temperature; (2) the solvent is virtually insoluble in water; (3) the solvent does not dissolve salts. The DSE process, which is explained in Figure 1, is based on liquid-liquid extraction; the solubility of water in the directional solvent as temperature increases (thermoresponsiveness), which enables simple regeneration. These features given DSE several distinct advantages compared to existing technologies: (1) DSE is membrane-free and thus is not restricted by membrane fouling concerns for high salinity water; (2) DSE operates in the liquid state, which reduces the size and complexity of the equipment; (3) DSE can be paired with a low-temperature renewable heat source (e.g., low-cost thermal solar).

Amines [27] and alcohols [28] were explored over fifty years ago as the first directional solvents for desalination. These solvents can only treat low salinity water (5000 ppm) and have a high solubility in water, leading to high solvent losses [29]. In the 1990s, The Puraq Company proposed a liquid polymers-based [30, 31] directional solvent, which was commercially unsuccessful due to elevated solvent production costs [32], although recent work by Thanaplan *et al.* [33] reexamines the energetics of the Puraq Company's process. Recently, Luo and co-workers proposed fatty acids, including decanoic acid ($CH_3(CH_2)_8COOH$) and octanoic acid ($CH_3(CH_2)_6COOH$) as directional solvents. The highly polar C=0 and O−H groups in the fatty acids facilitate the formation of hydrogen bonds with water molecules, which enables carboxylic acids to dissolve water. However, the chain end is hydrophilic, which helps ensure the solubility of the acids in water is negligible (30 - 150 ppm) [15]. In recent work, Guo *et al.* [34] proposed the use of ionic liquids, which have a greater thermoresponsivness ability and a solubility comparable to fatty acids. In this work, we will assess the technoeconomic potential of fatty acid and ionic liquid directional solvents in the context of an optimized DSE process.

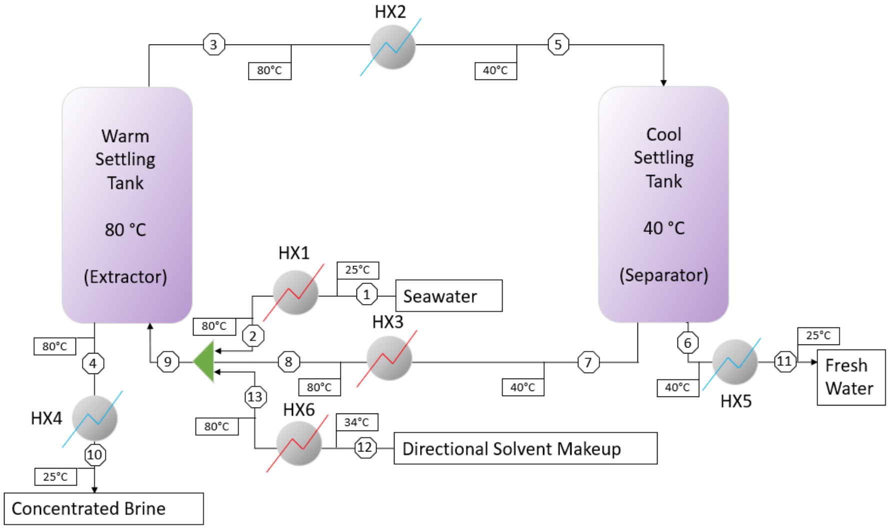

Figure 1: Illustration of the basic directional solvent extraction (DSE) process. Seawater (stream 1) is heated to the maximum allowable temperature (80°C is shown) in the process and mixed with the directional solvent (stream 8). The mixed emulsion of water and directional solvent (stream 9) settles in the warm settling tank. Water dissolves in the directional solvent, and concentrated brine (stream 4) is extracted from the mixture by gravity. The directional solvent and dissolved water (stream 3) are then cooled down. Freshwater is expelled from the mixture and decanted (stream 6). Decanoic acid is reheated and recycled (stream 8). A small amount of directional solvent dissolves in the freshwater and is lost (stream 6). Thus a small directional solvent make-up feed is added to the system (stream 12) to ensure steady-state operation.

3.2.1. Effectively utilize low-grade heat and no/limited membrane costs

Luo and co-workers [14, 15, 13, 16, 17, 18] recently demonstrated octanoic and decanoic acid can efficiently desalinate water. Specifically, they experimentally observed the solubility of water in decanoic acid changes from 3.8 wt% at 34°C to 5.9% at 80°C, with negligible solubility of fatty acid in water [16]. This thermoresponsive characteristic of the directional solvent enables thermal regeneration and is essential to the DSE process. Lou and co-workers then demonstrated the DSE concept in a continuous bench-scale process, successfully extracting 2.5 gals of freshwater per day from a 700 ppm -1100 ppm salinity feed (0.07-011 wt%) utilizing octanoic acid [16]. Based on these experiments, they estimated a total energy consumption of 184 kW/m^3 for decanoic acid and 101 kWh/m^3 for octanoic acid, assuming heat integration with 90% heat exchanger efficiency[16].

3.2.2. Demonstrated performance for higher salinities

Bajpayee *et al.* [14] demonstrated the effectiveness of octanoic acid to treat salty brines from 3,667 ppm to 58,333 ppm TDS (total dissolved solids). Likewise, they successfully treated saturated brines show water extraction with DSE of brine with 290,000 ppm (NaCl) [14]. These results are promising for DSE to treat produced water with high TDS from oil and gas extraction (up to 460,000 ppm).

3.2.3. Scope for molecular-to-systems optimization

There are vast unexplored opportunities to optimize DSE across molecular and process scales. Existing fatty solvents require ≈90 m^3 of recycle per 1 m^3 of freshwater, which makes the processes remain energy-intensive. Alotaibi *et al.* [16] performed heat integration for a single-stage continuous process for DSE utilizing octanoic and decanoic acids using flowrates obtained from bench-scale experiments [16]. Their analysis used the transshipment heat integration model, which assumes fixed flowrates and temperatures [35]. While insightful, this analysis technique often overlooks opportunities to reduce energy intensity that are only realizable by simultaneously optimizing process conditions (flowrates, temperatures, compositions) and performing heat integration [36]. In this work, we show the benefits of more extensive process optimization. At the molecular scale, Guo *et al.* [34] recently measured the thermophysical properties of a handful of ionic liquids as candidate directional solvents. However, there are well over a billion candidate solvents to consider. In this work, we use rigorous process modeling and optimization to set quantitative solvent thermophysical property targets as a means to narrow the vast molecular design space.

4. Methods: thermoeconomic optimization framework

As a first step to realize molecular-to-system optimization of the DSE platform, we propose a computational framework for bottom-up rapid screening of candidate solvent and top-down identification of continuous solvent properties. In this section, we fully define the mathematical models and computational implementation.

4.1. Problem statement

Given inlet water salinity (e.g., 35,000 ppm NaCl), water rejection ratio (e.g., 50% water rejection rate), physical properties of the directional solvent, and a maximum temperature of the heat input, *manipulate* the temperature and material flows in the DSE process (streams in Figure 1) to *minimize* the specific energy of the problem. We formulate this as a nonlinear optimization problem (M1):

min	Specific Thermal Energy	
s.t.	Unit Operation Models	Table 3
	Embedded Heat Integration	Eq. (4)-(10)
	Physical Bounds	
	50% Water Rejection Rate	
	Inlet Water Specification (Seawater)	

We use variations of the optimization problem (M1) for both bottom-up screening and top-down analysis. We adopt an equation-oriented (EO) approach, wherein all of the process specifics and governing engineering phenomena (e.g., thermodynamics, equipment performance, energy costs, etc.) are expressed as mathematical equations that are simultaneously converged during optimization. This approach is extremely flexible. It naturally accommodates variable bounds and facilitates embedded heat integration during the optimization procedure. (M1) is a nonconvex optimization problem with 77 linear equality constraints, 26 nonlinear equality constraints, 6 linear inequality constraints, 6 nonlinear equality constraints, 30 quadratic equality constraints, and 136 variables. Using the Julia [37] and JuMP [38] computational environment, we can efficiently solve (M1) using IPOPT solver [39] and HSL (MA27) [40] in approximately 0.2 seconds after thoughtful initialization. The remainder of this section describes all of the mathematical equations and input data used in (M1).

4.2. Unit Operation Models

The DSE process is a collection of tanks, heat exchangers, splitters, and mixers, as shown in Figure 1. These basic unit operations share a similar structure, as shown in Figure 2: each unit has one or more input streams and either one or two outlet streams. We utilize mass and energy balances and liquid-liquid equilibria expressions to calculate the outlet streams of the tanks. We assume the entire process operates at a steady-state, and there are no chemical reactions in the process. The equations for each unit operation are shown in Table 3.

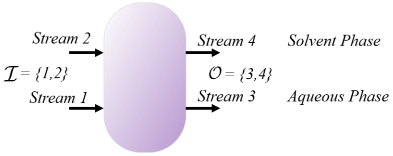

Figure 2: The tank, mixer, and single phase heat exchanger unit operations all share the same general equipment unit structure. Here sets $\mathcal{I}$ and $\mathcal{O}$ denote the inlet and outlet streams, respectively. Often, each outlet stream is designated either the solvent or aqueous phase.

4.2.1. Liquid-liquid phase separation

The DSE process relies on temperature varying solubility of water in the directional solvent. Unfortunately, temperature-dependent ternary phase data for water, solvent, and salt are not available in the literature. For preliminary process analysis, we assume the solubility of water in the solvent is linearly dependent on temperature shown in Eq. (1). We fit A and B via regression analysis using experimental data for the mixture decanoic acid, water, and salt from Bajpayee *et al.* [14] and Oliveira *et al.* [41] for the mixture decanoic acid and water. Figure 3 shows this simple model fits the data well. Fitted parameters

Table 3: Mathematical model for each unit operation in the DSE process. F is the molar flow (kmol/s). x are the molar fractions of the components $\mathcal{C}$ which include the solvent, water and salt. All of these component exist in the solvent *1* and the aqueous/salty *2* phases. T is the temperature (K) and C_p is the heat capacity (J/mol-K). Subscripts *in* and *out* denote inlet and outlets streams, respectively, for each piece of equipment.

Equation	Tanks	Isothermal mixer	Single phase heat exchanger
Overall mass balance	$F_{in} = \sum_{j\in\{1,2\}} F_j$	$\sum_{i\in in} F_{in} = F_{out}$	$F_{in} = F_{out}$
Overall component balance	$F_{in}x_{in,c} = \sum_{j\in\{1,2\}} F_j x_{j,c} \quad \forall c \in \mathcal{C}$	$F_{in}x_{in,c} = \sum_{j\in\{1,2\}} F_j x_{j,c} \quad \forall c \in \mathcal{C}$	$x_{in,c} = x_{out,c} \quad \forall c \in \mathcal{C}$
Equilibrium equation	$x_w = A + BT$		
Summation equation	$\sum_{c\in\mathcal{C}} (x_{1,c} - x_{2,c}) = 0$		
Energy Balance	$T_{in} = T_{out}$	$T_{in} = T_{out}$	$Q = C_p F_{in}(T_{out} - T_{in})$

are reported in Table 4. We approximated the solubility in the aqueous phase by assuming the solubility of the acid and salt as constant with the values of the compositions at 35°C and are shown in Table 5.

$$x_w = A + BT \tag{1}$$

However, the combination of values that A and B can take are limited as x_w has values between 0 and 1 mol/mol. We determine the physical solutions to (M1) between the maximum allowable temperature of the DSE process (T_{max}) and the minimum process temperature T_{min}.

$$0 \leq A + BT_{max} \qquad 1 \geq A + BT_{max} \qquad 0 \leq A + BT_{min} \qquad 1 \geq A + BT_{min} \tag{2}$$

4.2.2. Single-phase heat exchanger

The heat duty in the heat exchanger is $Q = C_p F_{in}(T_{out} - T_{in})$, where C_p is the heat capacity, F_{in} is the flowrate, and $T_{out} - T_{in}$ is the temperature

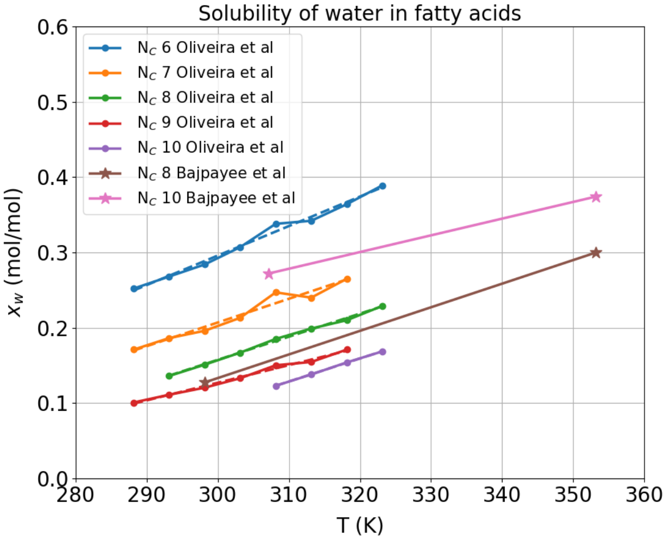

Figure 3: We perform linear regression on solubility to calculate the temperature swing (thermoresponsiveness) of the solubility of water in the carboxylic acid (solvent phase) using two sets of experimental data. Bajpayee *et al.* [14] provides data for ternary mixtures C_8 and C_{10} fatty acids, water, and salt. Oliveira *et al.* [41] provides data for binary mixtures of C_6 to C_{10} fatty acids and water.

difference. We calculate C_{pi} for the organic solvent i with the capacity group contribution method [43]:

$$C_{pi} = \sum_{k \in G} N_k (A_k + B_k t) \qquad t = T/1000 \tag{3}$$

Eq. (3) captures the influence of N_k times of functional group k appears in the organic component i. For water we use coefficients given in Table 7[43]:

$$C_{pi} = A + Bt + Ct^2 + Dt^3 + E/t^2, \qquad t = T/1000 \tag{4}$$

$$\tag{5}$$

and for the ionic liquid, we use coefficients given in Table 7 and Eqs. (6) [44].

$$C_{pi} = A + BT \tag{6}$$

Table 4: Coefficients for the equation $x_w = A + BT$ for solubility correlation for carboxylic acids and [emim][Tf_2N][34].

Bajpayee *et al.* [14]

Number of carbons	**A (mol/mol)**	**B (mol/mol K)**
8	-0.8304	0.0032
10	-0.4091	0.0022

Oliveira *et al.* [41]

Number of carbons	**A (mol/mol)**	**B (mol/mol K)**
6	-0.5731	0.0039
7	-0.7618	0.0031
8	-0.7367	0.0031
9	-0.5743	0.0023
10	-0.8187	0.0036

Ionic liquid	**A (mol/mol)**	**B (mol/mol K)**
[emim][Tf_2N]	-1.3417	0.0063

Table 5: Solubility of carboxylic acids in water [42]

Acid	**N_c**	**Solvent solubility in water (mol/mol)**	**Solubility in water [ppm]**
Hexanoic	6	1.678E-3	10,820
Heptanoic	7	3.348E-4	2,419
Octanoic	8	8.495E-5	680
Nonanoic	9	3.416E-5	300
Decanoic	10	1.339E-5	128
Ionic Liquid		**Solvent solubility in water (mol/mol)**	**Solubility in water [ppm]**
[emim][Tf_2N]		5.985E-6	300

We then calculate the C_p of each stream (mixtures) using the the component heat capacities C_{pi} and the mole fractions x_i: 215

$$C_p = \sum_{i \in C} C_{pi} x_i \tag{7}$$

The heat capacity of NaCl is considered constant with a value of 15.058 J/mol-K

[43]. Coefficients for Eqs. (3)-(6) are given in Tables 6 and 7.

Table 6: Heat capacity parameters for group contribution method [43].

Functional group	**A**	**B**
	J/molK	J/mol-K^2
CH_3	14.5504	540.60
CH_2	19.539	32.21
COOH	-49.7595	421.11

Table 7: Heat capacity parameters for Eq. (4) [43] and Eq. (6) [44]. $C_{pi} = A + Bt + Ct^2 + Dt^3 + E/t^2$, $t = T/1000$ (J/mol-K).

Component	**A**	**B**	**C**	**D**	**E**
	(J/mol-K)	(J/mol-K*kK)	(J/mol-K*kK^2)	(J/mol-K*kK^3)	(JkK^2/molK)
H_2O	-203.6060	1583.29	- 3196.43	2474.455	3.855326
[emim][Tf$_2$N]	430.39	0.315	0	0	0

4.3. Embedded Heat Integration

We embed the heat integration equations from the Duran-Grossman formulation [45] directly into the process optimization problem. This allows us to simultaneously optimize the process operating conditions (flowrates, compositions, temperatures) while minimizing the thermal energy input per unit of freshwater product. In contrast, Alotaibi *et al.* [16] only perform heat integration for a fixed process operating conditions. We emphasize our approach is superior because it optimizes more degrees of freedom. The optimizer manipulates flowrates, compositions, and temperatures to balance complex interdependencies between temperature-dependent phase equilibria and the pinch point, which limits heat integration. For completeness, we now summarize the heat integration model.

Each single-phase heat exchanger half is designated as a hot stream (requires cooling) or a cold stream (requires heating), denoted with sets $\mathcal{S}_{\mathcal{H}}$ and $\mathcal{S}_{\mathcal{C}}$, respectively. We then consider the inlet of each heat exchanger as a pinch candidate temperature T^p and add the minimum driving force ΔT_{min} to the cold stream temperatures:

$$T^p = \begin{cases} T_p^{in} & \forall \quad p \quad \in \mathcal{S_H} \\ T_p^{in} + \Delta T_{min} & \forall \quad p \quad \in \mathcal{S_C} \end{cases} \tag{8}$$

We use the set $\mathcal{P} = \mathcal{S_C} \cup \mathcal{S_H}$ to denote all pinch candidate temperatures. For each pinch candidate $p \in \mathcal{P}$, we calculate the heat content above pinch temperature T^p:

$$QA_H^p = \sum_{i \in \mathcal{S_H}} FC_{pi}[\tilde{\max}(T_i^{in} - T^p) - \tilde{\max}(T_i^{out} - T^p)], \quad \forall p \in \mathcal{P} \tag{9}$$

Similarly, we calculate the heat content below pinch temperature T^p:

$$QA_C^p = \sum_{i \in \mathcal{S_C}} FC_{pi}[\tilde{\max}(T_j^{out} - T^p + \Delta T_{min}) - \tilde{\max}(T_i^{in} - T^p \Delta T_{min})], \quad \forall p \in \mathcal{P} \tag{10}$$

The minimum hot utility duty Q_S must be larger than the difference between the heat contents below and above each pinch candidate.

$$\underbrace{Q_S}_{\text{heating utility}} \geq \underbrace{QA_C^p}_{\substack{\text{heat contents above} \\ \text{pinch candidate}}} - \underbrace{QA_H^p}_{\substack{\text{heat contents below} \\ \text{pinch candidate}}} \quad \forall \quad p \in \mathcal{P} \tag{11}$$

Finally, we use an energy balance to calculate the minimum cold utility duty Q_W:

$$\underbrace{Q_W}_{\text{cooling utility}} = \underbrace{Q_S}_{\text{heating utility}} + \underbrace{\sum_{j \in \mathcal{S_C}} Q_j^{in}}_{\text{internal heating}} - \underbrace{\sum_{i \in \mathcal{S_H}} Q_i^{out}}_{\text{internal cooling}} \tag{12}$$

In order to keep the optimization problem differentiable, we used a smoothed approximation for the max operator:

$$\tilde{\max}(x) = \frac{1}{2}\left(\sqrt{x^2 + \epsilon^2}\right) \approx \max(x, 0), \qquad \epsilon^2 = 10^{-6} \tag{13}$$

This model is effective because the combinatorial search for the pinch candidate is cast as inequality constraint Eq. (11), which is efficiently handled in equation oriented process optimization.

4.4. Cost model

After solving (M1), we estimate equipment and operating costs and then calculate the price per unit of freshwater production.

The heat integration model described above only computes the minimum hot and cold utilities when solving (M1). As a post-processing step, we perform sequential optimization to design the heat exchanger network. We first solve a mixed integer linear program to predict matches to minimize the number of heat exchangers. We then solve a nonlinear program to calculate the heat exchanger areas.[35, 36]. Finally, we use Guthrie's Method [36] to calculate the equipment costs. We use the present cost index of December 2018 (613.6) and a straight-line depreciation:

$$ADE = \frac{(CotA - SV)}{ULA} \tag{14}$$

Here, ADE is the Annual Depreciation Expense, $CotA$ is the cost of the assets, SV is the salvage value after the useful life of the plant (20% of the cost of the assets), and ULA is the estimated useful life of the plant. We assume a cost of electricity of 0.05 \$/kWh (average price of Texas, Oklahoma, Lousiana, New Mexico, Georgia, and Utah) [46]. We assume a 2 psi pressure drop every 100 feet, and the heigh of the tanks is calculated for every process solution for pumping electricity. We assume a cost of heating utilities of 2.778 \$/GJ from waste heat, a similar cost to solid waste, coal, or nuclear energy [47]. We assume the system has a useful life of 20 years for cost calculations, and we selected stainless steel for the material of the equipment because the plant handles saline brines and freshwater. The cost of decanoic acid is set to 12 \$/kg [48].

5. Results: Bottom-up Process Optimization

We now solve the optimization problem (M1) in several bottom-up case studies to predict the best possible performance of candidate directional solvents in a fully optimization process. We first compare our optimized reference design with Alotaibi *et al.* [16]. Then, we perform a sensitivity analysis to quantify the impact of ΔT_{min} (heat exchanger size) and the maximum temperature (heat source quality). Finally, we compare candidate organic acid solvents.

5.1. Reference Design for Decanoic Acid Directional Solvent

We set the temperature bounds between 34°C and 80°C, specify a 50% reject ratio, and set $\Delta T_{min} = 6°\text{C}$[1] to match Altoabi *et al.* [16]. Results from solving (M1) are shown in Tables 8, 9, 10 and Figure 4. From the results, we draw these observations:

Observation A1. A considerable portion of the decanoic acid (128 ppm) is solubilized in the outlet of freshwater and salty brine. We calculate that, at steady-state, the process requires 10^{-4} kmol/s of make-up directional solvent. We emphasize this make-up was not considered by Alotaibi *et al.*[16], who based their process analysis pseudo-steady-state experimental data.

Observation A2. Our approach finds the same pinch point, 50°C, as shown in Altoabi *et al.* [16].

Observation A3. Solving (M1) predicts specific energy of 191 $\text{kW}_t\text{h/m}^3$ (kiloWatts per hour of thermal energy)of freshwater with decanoic acid as a solvent, whereas Alotaibi *et al.* [16] 180 $\text{kW}_t\text{h/m}^3$ of freshwater. We highlight two differences that can explain our 9% larger specific energy: first, the addition of a feed (make-up) stream of decanoic acid. Second, we cool down the solvent-water emulsion stream to 34°C (limiting temperature due to solvent crystallization) in contrast to the 40°C used by Alotaibi *et al.* [16].

Observation A4. Solving the cost analysis for treating 1 m^3 of water results in a cost of \$3.31 /m^3 of freshwater. The cost is high compared to modern technologies: between \$0.27 /m^3 and \$1.62 /m^3 of freshwater. Solvent loss has a significant influence on the cost of DSE desalination.

---

[1] Altoabi *et al.* [16] report a heat exchanger effectiveness of 90%, which we convert to ΔT_{min} = 6°C.

Table 8: Stream results for reference design with decanoic acid as solvent using 80°C as maximum allowable temperature ΔT_{min}=6°C. See Figure 1 for schematics. Flowrates are comparable to Table 3 in Alotaibi *et al.* [16].

Stream	**Flow**	**Temperature**	x_d	x_w	x_s
	kmol/s	°C	%mol	%mol	%mol
1	0.5	25	0.00	98.89	1.11
2	0.5	80	0.00	98.89	1.11
3	1.81	80	63.18	36.78	10^{-4}
4	0.25	80	10^{-3}	97.97	1.99
5	1.81	34	63.18	36.78	10^{-4}
6	0.25	34	10^{-4}	99.78	0.21
7	1.56	34	73.33	26.66	10^{-4}
8	1.56	80	73.33	26.66	10^{-4}
9	2.06	80	55.50	44.22	0.26
10	0.25	25	10^{-3}	97.97	1.99
11	0.25	25	10^{-4}	99.78	0.21
12	10^{-4}	34	100	0.00	0.00
13	10^{-4}	80	100	0.00	0.00

5.2. Sensitivity Analysis: Maximum Temperature and ΔT_{min}

Next, we considered the sensitivity of process designs to both the maximum temperature and ΔT_{min}, which controls the heat exchanger size and effectiveness. We solve (M1) with three different sets of experimental data as the LLE correlation input: decanoic acid-water data form Oliveira *et al.* [41], decanoic acid-water-salt from Bajpayee *et al.* [15], and [emim][Tf_2N]-water-salt from Guo *et al.* [34]. Figure 5 shows specific energy at six maximum temperature between 40 °C and 90 °C and ten different ΔT_{min} between 1 °C and 10 °C. Figure 6 shows specific energy at five maximum temperature between 35 °C and 75 °C and ten different ΔT_{min} between 1 °C and 10 °C. Solving (M1) 169 times to generate Figures 5 and 6 took less than 1 minute. From these results, we

Table 9: Heat exchanger sizes and temperatures for the reference design (decanoic acid as solvent, 80°C as maximum allowable temperature). More than 90% of the heating and cooling occurs in heat exchangers HX3 and HX2, respectively. This is due to the large amount of decanoic acid that gets recycled in the process to desalinate water at a 50% extraction ratio. For practical considerations, one may choose not to add HX6 due to the low heat duty of the heat exchanger and the small flow of solvent.

Heat exchanger	**Stream**		**Temp (°C)**		**Q (kWh)**
	Inlet	Outlet	Inlet	Outlet	
HX1	S1	S2	25	80	2.09
HX2	S3	S5	80	34	-23.44
HX3	S7	S8	34	80	23.00
HX4	S4	S10	80	25	-1.045
HX5	S6	S11	34	25	-0.17
HX6	S12	S13	34	80	3.2E-3

Table 10: Heat integration results for the reference design. QA_h is the heat exchanged above the pinch temperature and QA_c is the heat below the pinch temperature. Both streams S3 and S4 are at the pinch temperature of 50°C.

Heat exchanger	**Exchanger Inlet**	**Type of Stream**	**QA_h (kWh)**	**QA_c (kWh)**	**QA_c-QA_h (kWh)**
HX1	S1	Cold	24.03	24.31	0.28
HX2	S3	Hot	0.01	3.12	3.11*
HX3	S7	Cold	20.77	23.88	3.10
HX4	S4	Hot	0.01	3.12	3.11*
HX5	S6	Hot	23.88	24.17	0.28
HX6	S12	Cold	20.77	23.88	3.10

* Pinch temperature

Table 11: LCOW for three different directional solvents without consifering solvent recovery. Costs of thermal energy, pumping electricity and equipment are lower using ionic liquid. However the cost of the solvent make-up increases considerably.

Directional solvent	LCOW	Solvent cost		Electricity cost		Thermal energy cost		Equipment cost	
	$	$	%	$	%	$	%	$	%
Decanoic acid	3.30	1.03	31.21	0.31	9.39	1.92	58.18	0.04	1.21
Octanoic acid	4.13	2.48	60.05	0.20	4.85	1.42	34.38	0.03	0.73
[emim][Tf_2N]	43.03	42.60	99.02	0.07	0.17	0.34	0.78	0.01	0.03

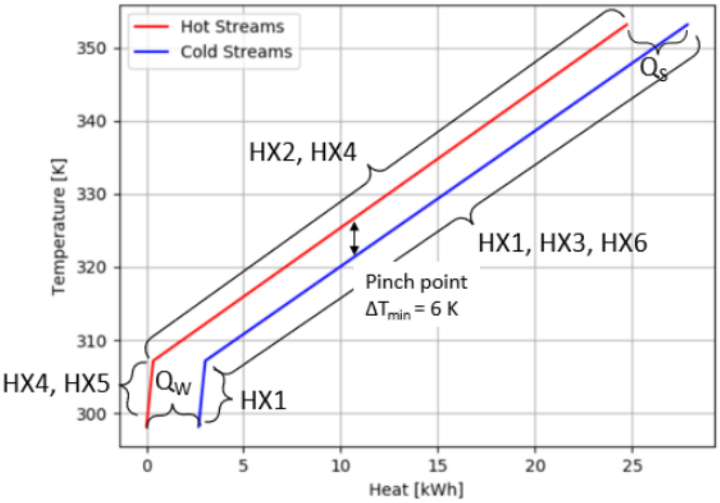

Figure 4: Composite curves for the reference design, including utilities. Most of the heat exchange is done in HX2 and HX3, which have the largest temperature difference and the highest flowrates. Recall HX1 heats inlet seawater to the temperature of the warm settling tank, HX2 cools the water-decanoic acid emulsion, and HX3 heats the recycled directional solvent. HX4 and HX5 cool the outlet concentrated brine and freshwater, respectively. Q_S and Q_W are defined as the minimum heating and cooling utility duties, respectively.

observe:

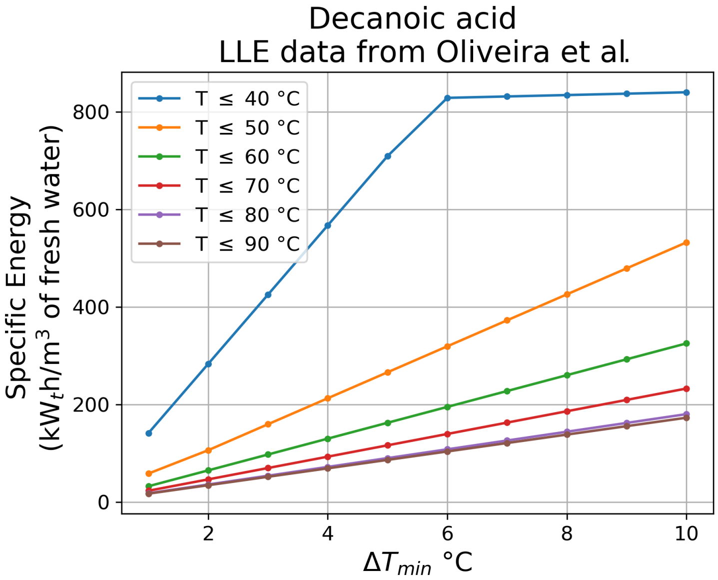

(a) Using data from Oliveira *et al.* [41]

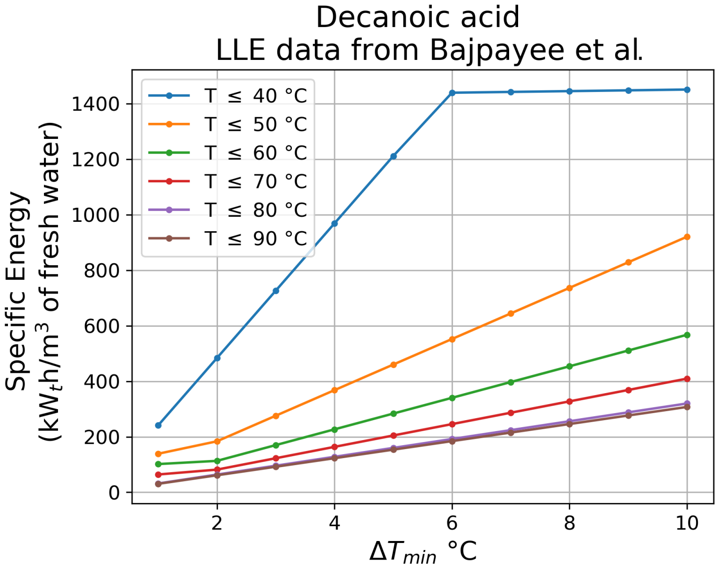

(b) Using data from Bajpayee *et al.* [15]

Figure 5: Sensitivity of specific energy to maximum temperature (heat source quality) and ΔT_{min} (heat exchanger size). Bajpayee *et al.* [15] data showed 2.6% more solubility of water in the solvent phase from Oliveira *et al.* [41]. The difference may be explained by the interaction of salt in the mixture. Higher maximum temperatures enable higher per pass extraction, which allows for a lower recycle flowrate and lower energy intensity. Solvents that enables higher per pass extraction at a lower temperature, the decrease in energy intensity would be higher. The specific energy difference between allowing (M1) to reach 80°C and 90°C is negligible. Heat exchangers with a temperature difference of less than 3°C are to achieve less than 50 kW$_t$h/m^3.

Observation B1. We find consistent trends with both sets of solubility data. Bajpayee *et al.* data[15] showed 2.6% more solubility of water in the solvent phase, which leads to 2 times lower energy-intensive process as the process needs fewer extractions per pass. The difference between the solubilities is because Oliveira *et al.* only considered binary water-acid mixtures.

Observation B2. As expected, higher maximum temperatures enable higher per pass extraction, which allows for a lower recycle flowrate (1.81 kmol/s for a maximum allowable temperature of 80°C, compared to 4.91 kmol/s for a maximum allowable temperature of 50°C) and lower energy intensity. This suggests that manipulating the solvent chemistry to increase the per pass extraction at a lower temperature will decrease the energy intensity.

Observation B3. The specific energy difference between temperature $\leq$80°C and $\leq$90°C is negligible. This is because increasing the pass per extraction increases the fraction of water in the solvent-water emulsion, which decreases the C_p of the mixture. As the amount of heat required to heat the mixture decreases at a higher maximum allowable temperature, so does the specific energy of the process. This result emphasizes little benefit for heat sources greater than 80°C for off-the-shelf organic acid solvents.

Observation B4. Heat exchangers with a temperature difference of less than 3°C are likely required to achieve less than $50\text{kW}_t\text{h/m}^3$ and 4°C to achieve less than $100\text{kW}_t\text{h/m}^3$ utilizing decanoic acid as a solvent. The heat exchangers would need to have an effectiveness of approximately 96% or higher to achieve the $50\text{kW}_t\text{h/m}^3$ goal utilizing decanoic acid.

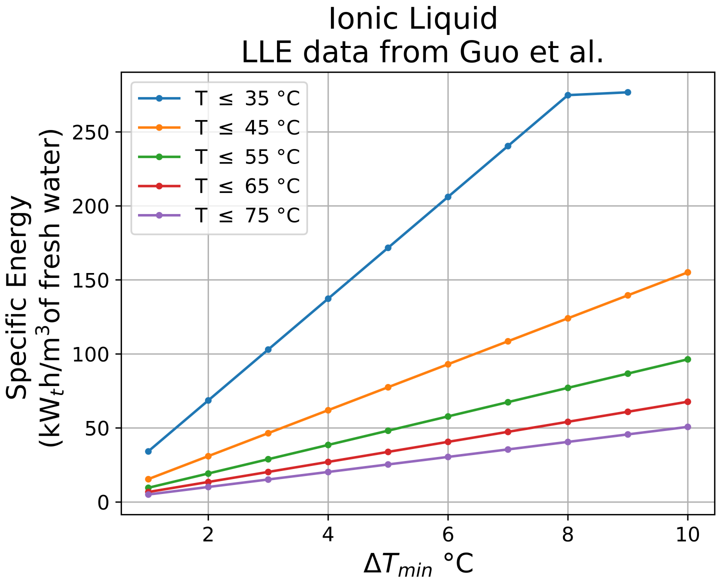

Figure 6: Effects of maximum temperature allowed for the process utilizing [emim][Tf$_2$N] as solvent. The specific energy of the process is greatly reduced compared to carboxylic acids.

Observation B5. We observe the IL the solvent [emim][Tf$_2$N] can achieve 50 kW$_t$h/m^3 using maximum allowable temperature of 65°C and ΔT_{min} of 6°C. Our analysis shows that, from an energetics perspective, ILs are a more promising class of directional solvents.

5.3. Sensitivity Analysis: Length of the Chain of Carboxylic Acids

We now rapidly screen five carboxylic acids as directional solvents. We solve (M1) using acid-water mixture data for Oliveira *et al.* [41]. We set the amount of acid dissolved in the aqueous phase as the solubility of the fatty acid at 20°C, shown in Table 5. The minimum temperature for the process is set as the larger of the melting temperature of the acid or 25°C at ambient temperature. The 120 instances of (M1) shown in Figure 7 were solved in approximately 25 seconds total. From the results, we observe:

Observation C1. In Figure 3, we see there is not a clear relationship between the solubility of water in organic acid and the length of the carbon chain. However, we find the slope A, i.e., the thermoresponsiveness of solubility, is most influential on specific energy.

Observation C2. For solvent selection, the three most important factors are i) the change in water solubility for a fixed temperature change (thermoresponsiveness); ii) the melting temperature of the fatty acid, which limits the minimum operating temperature; and iii) the solubility of the directional solvent in freshwater.

Observation C3. Similar to observation B4, high-performance heat exchangers are required to achieve less than 50 $\mathrm{kW}_t\mathrm{h/m}^3$ using C_6 to C_{10} fatty acids

Observation C4. The cost of the process increases with the length of the carboxylic acid chain. The solvent solubility in water decreases as the carbon chain increases, diminishing the amount of solvent loss and the solvent make-up cost in the process.

Observation C5. DSE process using fatty acids are not economically viable, with a best-case scenario of \$1.29 per m^3 of freshwater for decanoic acid with heat exchangers with ΔT_{min} of 1°C.

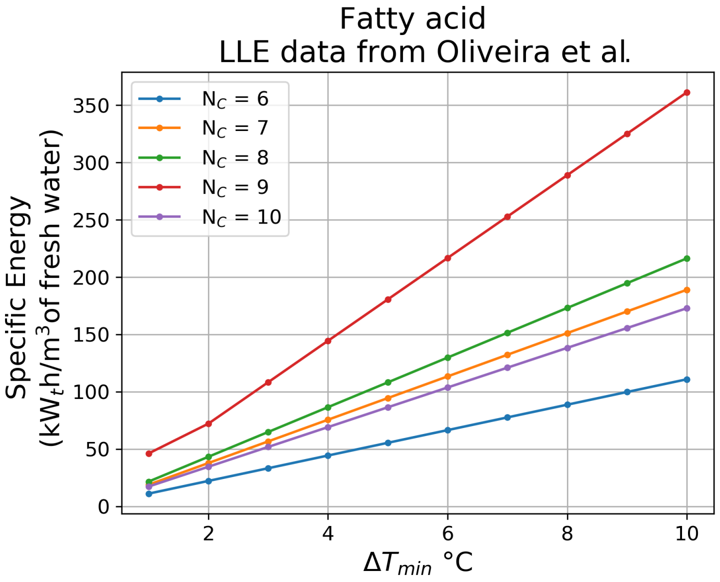

(a) Effects on specific energy using different carboxylic acids as the DS.

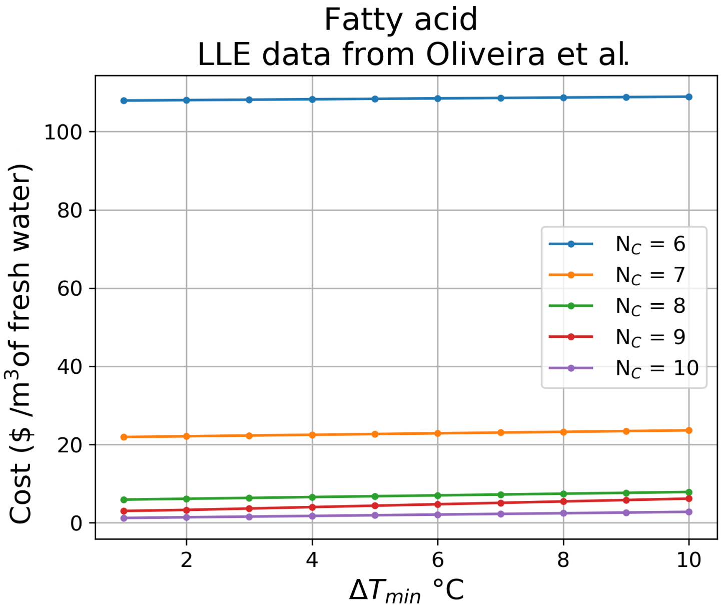

(b) Effects on the cost of the DSE process utilizing C_6 to C_{10} fatty acids.

Figure 7: There is not a clear influence in the length of the chain of carbons (N_c) in the energy required for the separation and the cost of the process. DSE remains energy intensive utilizing any C_6 to C_{10} carboxylic acid and suffers from solvent lost. The cost of the process increases with the increase of solubility of the solvent in water. The values of the cost at utilizing a ΔT_{min} from 1°C to°C 10 for different carboxylic acids are: for $N_c = 6$: $107.91-108.99 per m^3, for $N_c = 7$: $21.91-23.55 per m^3, for $N_c = 8$: $5.90-7.86 per m^3, for $N_c = 9$: $3.00-6.18 per m^3, for $N_c = 10$: $1.29-3.79 per m^3. see Table 5 for specific quantities of solvent loss.

6. Results: Top-Down Solvent Property Targets

Based on the bottom-up analysis in Section 5, we conclude that known carboxylic acids are not an economical solution for directional solvent extract. Although [emim][Tf_2N] is, from an energetic perspective, a more promising directional solvent. Limited data for IL-water-salt mixtures prevents bottom-up screening of more candidate IL solvents.

In this section, we generalize the optimization problem to consider hypothetical directional solvent molecule parameterized by two continuous properties: solubilities in the aqueous and solvent phases $x_{2,d}$, and $x_{1,w}$, and cost of the solvent. Thus we perturb 4 parameters in the technoeconomic analysis: A, B, cost and, the fixed value of $x_{2,d}$ leaving the warm settling tank. We then perform top-down sensitivity analysis to identify **idealized directional solvent property targets** to add in molecular discovery. This continuous processing is a precursor to discrete molecular optimization [49].

6.1. Top-Down Analysis: Carboxylic Acids

We start by performing a sensitivity analysis for hypothetical carboxylic acid solvents. For each set of properties, we first solve (M1) to compute flowrates and temperatures that minimize specific energy. We then estimate the cost of each design, including the cost of solvent make-up. We repeat this procedure 10,000 times, changing three basic properties: 1) the thermoresponsiveness of the solubility of the solvent (A), 2) the amount of water that solubilizes in the solvent at a reference temperature (B), and 3) the amount of solvent dissolved in the freshwater at the outlet of the DSE process ($x_{2,d}$). We calculate the 10,000 costs in the feasible region, determined by Eqs. (2). From the results shown in Figure 8, we conclude:

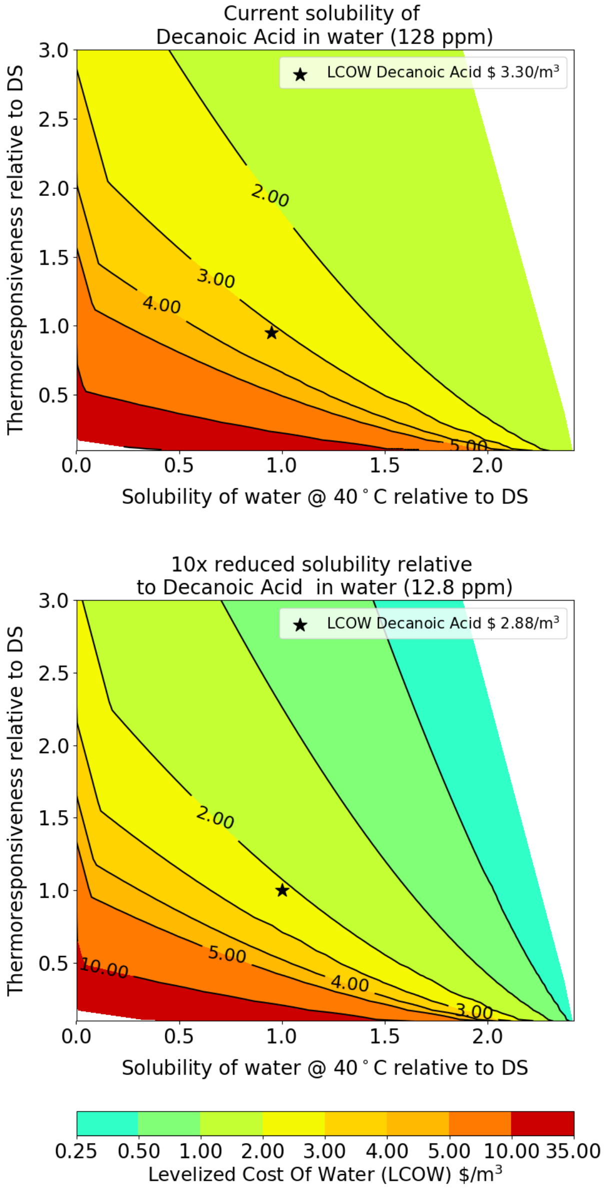

Figure 8: Due to the low cost of decanoic acid ($12/kg), thermoresponsivness (A), and the solubility of water (B) factors in costs. (Top) Current solubility of the solvent in water. The thermoresponsive ability influences the recycle ratio, which accounts for most of the heat and electricity required and the equipment's size. (Bottom) Reducing the solubility of the solvent in water would improve the price of the process. However, an improvement in thermoresponsivness would still be needed.

Observation D1. Thermoresponsive ability (A), and low solubility of the solvent in water ($x_{2,d}$) are the properties most influential of the DSE process's LCOW. Increasing the base solubility of water in the solvent (B) reduces the recycle ratio by decreasing the amount of solvent needed for water to dissolve. For decanoic acid, we calculate \$3.30/m^3 of freshwater and \$4.13/m^3 of freshwater for octanoic acid. Even though the energy cost utilizing octanoic acid as the solvent is lower than using decanoic acid (\$2.20/m^3 of freshwater for decanoic acid and \$1.62/m^3 of freshwater for octanoic acid), the LCOW is higher because of the higher solubility of the solvent resulting in higher solvent make-up cost. Results show that by doubling thermoresponsive ability and reducing the solubility of the solvent in water by a factor of ten with respect to decanoic acid, can make DSE economical competitive with modern seawater desalination technologies (\$0.50 /m^3).

Observation D2. The recycle ratio is reduced as the thermoresponsive ability (A) of the solvent and the base solubility of water in the solvent (B) increase. This reduces the thermal and electric energy required to heat, pump, and cool the recycle of the DSE-water emulsion. Reducing the recycle ratio also drastically shrinks the size of the equipment. For example, increasing the thermoresponsiveness of the solvent by a factor of 2 decreases the recycle ratio by a factor of 20, which decreases the heat and electricity costs from \$2.20 per m^3 of freshwater to \$0.21 per m^3 of freshwater, and decreases equipment sizes by 400%.

Observation D3. Low solubility of the solvent in water decreases the solvent loss in the system and the cost associated with it. We found the directional solvent's solubility must be less than 10 ppm (assuming prices similar to decanoic acid) to reach a target of \$ 0.50 per m^3 of freshwater.

6.2. Top-down Analysis: Ionic Liquids

Next, we perform a sensitivity analysis for hypothetical IL directional solvents. Compared to carboxylic acids, ILs are a less mature chemical technology. We consider a current benchmark price of \$1,000/kg of [emim][Tf$_2$N] [50]. However, many expect economies of scale to dramatically reduce the cost of ILs as the market for these solvents grows. For example, Shiflett *et al.* [51] shows a price reduction of 92% for $[C_2MIM]^+[Ace]^-$ and 90% for $[C_2MIM]^+[BF_4]^-$. For the sensitivity analysis, we consider three IL costs: \$1,000/kg, \$100/kg, and \$10/kg. Due to these comparatively high costs, solvent loss is especially important for ILs compared to carboxylic acids. Thus, it is desirable to consider solvent recovery systems, such as a membrane for post-treatment.[2] For simplicity, we consider the complete recovery of the solvent from the freshwater feed product, which can be recovered with a nanofiltration polishing step.

---

[2] IL recovery from the freshwater stream is achievable with off-the-shelf filtration systems. Post-treatment for the brine reject is much more challenging due to concerns of membrane fouling. Full costing of the freshwater post-treatment system is beyond the scope of this work. Instead, we neglect capital costs and energy usage. As such, the property targets are optimistic but informative.

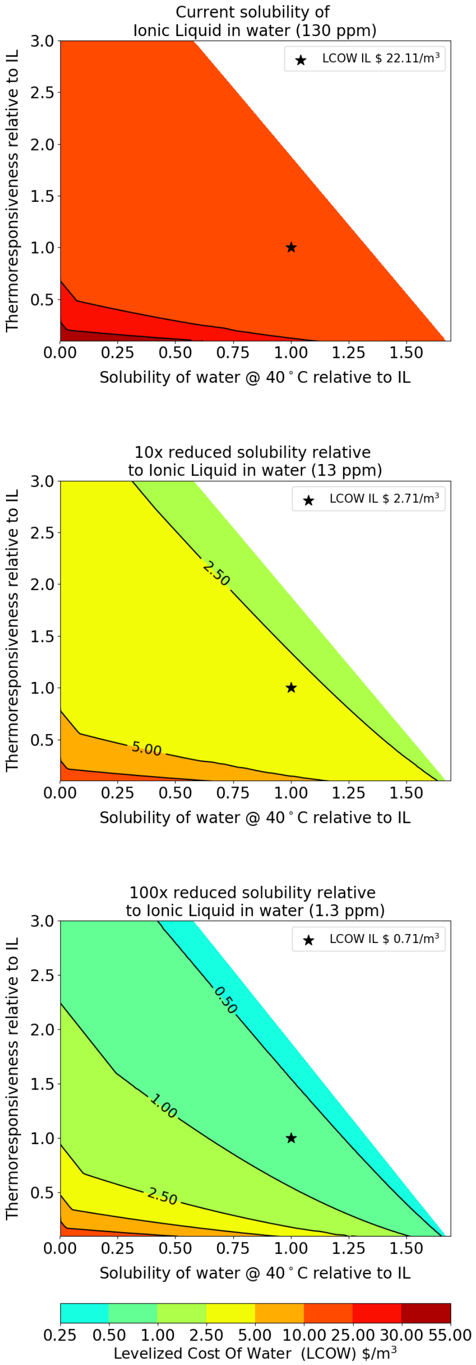

Figure 9: Cost of $1,000/kg of [emim][$Tf_2N$], it is not possible to achieve the LCOW of $0.50/m^3 of freshwater. In order to reach the desired LCOW the solubility of the solvent would need to be reduced by 100 times.

Observation E1. [emim][Tf_2N] is around 2 folds more thermoresponsive (A) than decanoic acid (0.0063 mol/mol/°C vs. 0.0022 mol/mol/°C). However, at the current price of the ionic liquid, the solvent loss ($x_{2,d}$) is critical. Figure 9 shows, a ten-fold reduction of solubility of the solvent in water ($x_{2,d}$) would lead to a LCOW of only 12% of the original cost. Improved thermoresponsiveness (A) alone is insufficient for ionic liquids have a competitive LCOW with carboxylic acids. Assuming the current price of ionic liquids, the solvent would still require a 100 fold reduction of the solvent solubility ($x_{1,d}$).

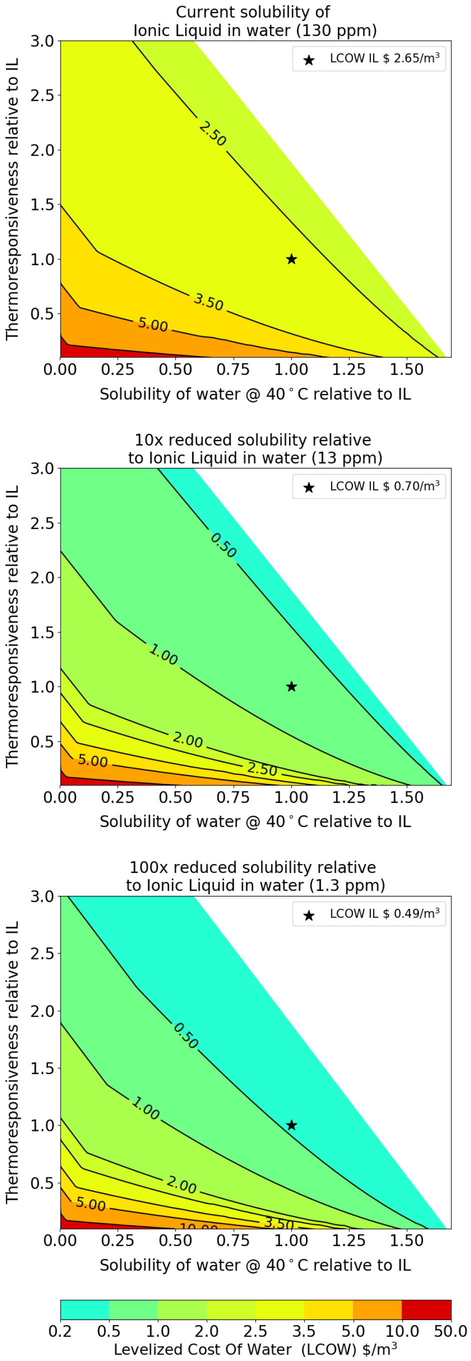

Figure 10: Sensitivy of LCOW with a cost of \$100/kg of [emim][Tf_2N]. (Top) With current solubility, the solvent loss would be too costly to achieve the required LCOW. (Bottom) With a ten-fold reduction of the solubility of the solvent in water, the solvent would require a 1.25 increase of solubility of water in the solvent or a 1.5 increase in thermoresponsiveness to achieve the LCOW of \$0.50/m^3 of freshwater. New unpublished data suggest a 4 ppm solvent loss in the salty brine.

Observation E2. Assuming a 90% cost reduction, the thermoresponsivness would need to be increased 1.5 times or the solubility of water 1.25 times. However, the solvent's solubility in water would need to be reduced by a ten-fold, as shown in Figure 9.

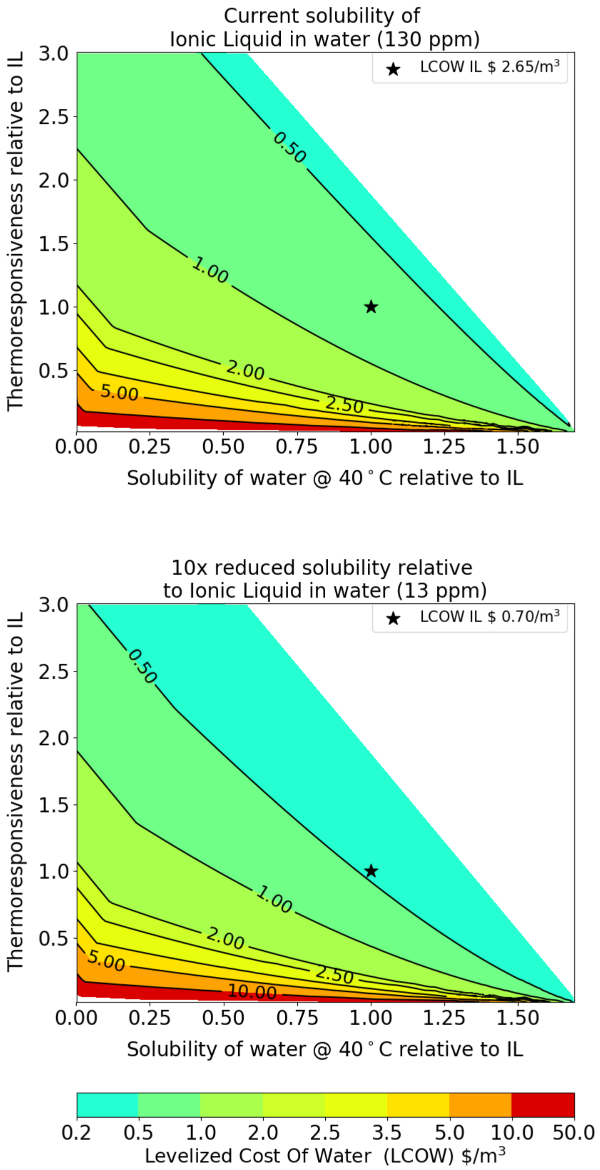

Figure 11: Sensitivy of LCOW with a cost of \$10/kg of [emim][Tf_2N]. (Top) With current solubility, the thermoresponsivness or the solubility of water would need to improve to achieve the required LCOW. (Bottom) With a 10 fold reduction of the solubility of the solvent in water we can achieve a LCOW of \$0.50/m^3 of freshwater.

Observation E4. For a cost of [emim][Tf_2N] of \$10/kg, the solvent solubility in water would have to be 10 times lower, and the goal of \$0.50/m^3 of freshwater would be achieved. However, it would still be possible to reach the target goal by increasing 1.2 the solubility of water in the solvent or increasing 1.5 the thermoresponsiveness.

Observation E5. For solvent with a cost as high as [emim][Tf_2N], the thermoresponsivness and the solubility of water in the solvent remain essential properties. With the current solvent solubility data, one would need to reduce the solvent loss at least ten times to utilize ionic liquids, even with a cost reduction of 99%. However, recent unpublished work suggests a 32-time reduction in solvent loss on the saline brine.

7. Conclusions and Future Work

Directional solvent extraction is a membrane-free, low-grade heat renewable desalination technology that can treat high salinity water resources. It can be paired with other technologies to create hybrid systems and can treat water at high concentrations of salts. In this work, we created a computational framework that facilitates the optimization of the process and rapid sensitivity analysis. Through these analyses, we found that higher maximum temperatures enable higher per pass extraction, which allows for a lower recycle flowrate and lower energy intensity. For solvent selection, we found that the length of the carbon chain has no apparent influence and that the most critical factors are the change in water solubility for a low-temperature swing (40°C-80°C), the melting temperature of the fatty acid, which limits the minimum operating temperature and the solubility of DS in freshwater. We believe that high-performance heat exchangers ($\Delta T_{min} \leq 3°C$) are likely required to achieve less than 50 $kW_t h/m^3$ using fatty acids. For current solubility data, we found we need a solvent that is twice as thermoresponsive as decanoic acid and ten times less soluble in water to get a cost-effective DSE process. Through sensitivity analysis of C_6 to C_{10} fatty acids, we have been able to show the limitations of fatty acids as directional solvents in the DSE process. The amount of thermoresponsiveness and the amount of solvent loss in the final product and concentrated brine make fatty acids a suboptimal solvent regarding the process's specific energy and total cost.

We have found ionic liquids such as [emim][Tf_2N] show promise as a solvent, as it reduced significantly the amount of thermal energy required for the process. However, the ionic liquid's price needs to be reduced to be an attractive, economical solvent for the process. The framework has proven to be able to rapidly evaluate the properties in which the ionic liquids would need to improve to achieve the LCOW of \$0.50/m^3. We have been able to determine that the most important properties depend on the solvent cost. We have set the quantitative targets at three price scenarios for ionic liquids and found the solubility of the solvent in water to become a determinant factor. As future work, we will elaborate on the framework to include process intensification (stage configuration, nanofiltration for solvent loss, electrocoalescer). We also need to verify and validate process models with experimental data.

The Edisonian search for new solvents has been slow. As future work, we plan to leverage computer-aided molecular design (CAMD) approaches [52, 53, 54] to realize holistic molecular-to-systems optimization of direction solvents and processes[55]. This includes refining and validating the process models, especially phase equilibria predictions, with additional experimental data. We ultimately see computational molecular and process scale modeling greatly accelerated the search for economically viable directional solvents. We also plan to explore the opportunities and costs of coupling DSE with inexpensive solar heating for sustainable and distributed desalination.

Nomenclature

Sets and indices

$\mathcal{C}$	Components (directional solvent, water, salt)	$c \in \mathcal{C} = \{d,w,s\}$
N_c	Number of carbons	$n \in N = \{6,7,8,9,10\}$
G	Functional Groups	$k \in K = \{CH_3, CH_2, H_2O, COOH\}$
sol	Solvent phase	
aq	Aqueous/salty phase	
in	Equipment inlet	$i \in I$ {inlet streams}
out	Equipment outlet	$j \in O$ {outlet streams}
N_k	Number of functional groups k	
P	Pinch candidates	$p \in P$

Variables

x	Molar fraction	
T	Temperature	K
Q_S	Heat from hot utility	kWh
Q_W	Heat from cold utility	kWh
Q_A	Total heat content above the candidate pinch	kWh
C_p	Heat capacity	J/mol-K
F	Molar flow	kmol/s

Parameters

ΔT_{min}	Heat Recovery Approach Temperature	K

Abreviations

DSE	Directional Solvent Extraction
MED	Multi-Effect Distillation
MSF	Multi-Stage Flash
RO	Reverse Osmosis
DS	Directional Solvent
ADE	Directional Solvent
$CotA$	Cost of Assets
SV	Salvage Value
ULA	Usefull Life os Assets
$LCOW$	Levelized Cost of Water

[1] EPA, How we use water.
URL `https://www.epa.gov/watersense/how-we-use-water#Daily%20Life`

[2] M. M. Mekonnen, A. Y. Hoekstra, Sustainability: Four billion people facing severe water scarcity, Science Advances 2 (February) (2016) 1–7. `doi:10.1126/sciadv.1500323`.

[3] M. Kummu, J. H. Guillaume, H. De Moel, S. Eisner, M. Flörke, M. Porkka, S. Siebert, T. I. Veldkamp, P. J. Ward, The world's road to water scarcity: Shortage and stress in the 20th century and pathways towards sustainability, Scientific Reports 6 (December) (2016) 1–16. `doi:10.1038/srep38495`.

[4] UNDESA, International Decade for Action "Water for Life" 2005-2015.
URL `https://www.un.org/waterforlifedecade/scarcity.shtml`

[5] N. Voutchkov, Energy use for membrane seawater desalination current status and trends, Desalination 431 (2018) 2–14.

[6] L. Atkinson, L. Bass, Produced Water Report: Regulations, Current Practices, and Research Needs, Groundwater Protection Council.

[7] J. E. Miller, Review of water resources and desalination technologies, 2003-0800, Sandia National Laboratories (March) (2003) 1–54.

[8] M. Elimelech, W. A. Phillip, The future of seawater desalination: Energy, technology, and the environment, Science 333 (6043) (2011) 712–717. `doi:10.1126/science.1200488`.

[9] L. Yang, I. E. Grossmann, J. Manno, Optimization models for shale gas water management, AIChE Journal 60 (October) (2014) 3490–3501. `doi:10.1002/aic.14526`.

[10] L. Yang, R. Salcedo-Diaz, I. E. Grossmann, Water network optimization with wastewater regeneration models, Industrial & Engineering Chemistry Research 53 (45) (2014) 17680–17695. `doi:10.1021/ie500978h`.

[11] E. Jones, M. Qadir, M. van Vliet, V. Smakhtin, S.-m. Kang, The state of desalination and brine production: A global outlook, Science of The Total Environment 657 (2019) 1343–1356. `doi:10.1016/j.scitotenv.2018.12.076`.

[12] K. R. Zodrow, Q. Li, R. M. Buono, W. Chen, G. Daigger, L. Dueas-Osorio, M. Elimelech, X. Huang, G. Jiang, J.-H. Kim, B. E. Logan, D. L. Sedlak, P. Westerhoff, P. J. J. Alvarez, Advanced materials, technologies, and complex systems analyses: Emerging opportunities to enhance urban water security, Environmental Science & Technology 51 (18) (2017) 10274–10281. `doi:10.1021/acs.est.7b01679`.

[13] T. Luo, A. Bajpayee, G. Chen, Directional solvent for membrane-free water desalinationa molecular level study, Journal of Applied Physics 110 (5) (2011) Article 054905. `doi:10.1063/1.3627239`.

[14] A. Bajpayee, Directional Solvent Extraction Desalination (PhD thesis), Massachusetts Institute of Technology (MIT).

[15] A. Bajpayee, T. Luo, A. Muto, G. Chen, Very low temperature membrane-free desalination by directional solvent extraction, Energy Environ. Sci. 4 (2011) 1672–1675. `doi:10.1039/C1EE01027A`.

[16] S. Alotaibi, O. Ibrahim, S. Luo, T. Luo, Modeling of a continuous water desalination process using directional solvent extraction, Desalination 420 (2017) 114–124. `doi:10.1016/j.desal.2017.07.004`.

[17] S. Luo, J. C. Eng, P. Technol, S. Luo, Y. Pang, T. Luo, A Continuous Directional Solvent Extraction Desalination Process Realized with the Aid of Electro-coalescence, Journal of Chemical Engineering 9 (4) (2018) Article 1000392. `doi:10.4172/2157-7048.1000392`.

[18] S. Alotaibi, O. Ibrahim, Y. Wang, T. Luo, Exergy analysis of directional solvent extraction desalination process, Entropy 321 (2019) 321. `doi:10.3390/e21030321`.

[19] World Bank, The Role of Desalination in an Increasingly Water-Scarce World, World Bank, Washington, DC.`doi:10.1596/31416`.

[20] T. V. Bartholomew, L. Mey, J. T. Arena, N. S. Siefert, M. S. Mauter, Osmotically assisted reverse osmosis for high salinity brine treatment, Desalination 421 (2017) 3–11, the Latest Advances and Opportunities in Forward Osmosis. `doi:10.1016/j.desal.2017.04.012`.

[21] T. V. Bartholomew, M. S. Mauter, Computational framework for modeling membrane processes without process and solution property simplifications, Journal of Membrane Science 573 (2019) 682–693. `doi:10.1016/j.memsci.2018.11.067`.

[22] G. Thiel, E. Tow, L. Banchik, H. W. Chung, J. Lienhard, Energy consumption in desalinating produced water from shale oil and gas extraction, Desalination 366 (2015) 94–112. `doi:10.1016/j.desal.2014.12.038`.

[23] K. S. Spiegler, Y. M. El-Sayed, A Desalination Primer: Introductory Book for Students and Newcomers to Desalination, Balaban Desalination Publications, 1994.

[24] S. Loutatidou, H. A. Arafat, Techno-economic analysis of med and ro desalination powered by low-enthalpy geothermal energy, Desalination 365 (2015) 277–292. `doi:10.1016/j.desal.2015.03.010`.

[25] K. C. Ng, K. Thu, S. J. Oh, L. Ang, M. W. Shahzad, A. B. Ismail, Recent developments in thermally-driven seawater desalination: Energy efficiency improvement by hybridization of the med and ad cycles, Desalination 356 (2015) 255–270. `doi:10.1016/j.desal.2014.10.025`.

[26] R. S. El-Emam, I. Dincer, Thermodynamic and thermoeconomic analyses of seawater reverse osmosis desalination plant with energy recovery, Energy 64 (2014) 154–163. `doi:10.1016/j.energy.2013.11.037`.

[27] R. R. Davidson, W. H. Smith, D. W. Hood, Structure and amine-water solubility in desalination by solvent extraction., Journal of Chemical & Engineering Data 5 (4) (1960) 420–423. `doi:10.1021/je60008a005`.

[28] G. C. Johnson, Recovery of potable water from sea and brackish, U.S. Patent 3,823,000A.

[29] C. B. Ellis, N. D. A, Fresh water from the ocean for cities, industry, and irrigation, Ronald Press Co.

[30] L. Lazare, The puraq seawater desalination process, Desalination 42 (1) (1982) 11–16. `doi:10.1016/S0011-9164(00)88736-6`.

[31] L. Lazare, The puraq seawater desalination process - an update, Desalination 85 (3) (1992) 345–360. `doi:10.1016/0011-9164(92)80016-3`.

[32] Lack of money to develop solvent extraction desalting plant, Water Desalination Report 6 (2).

[33] K. Thanapalan, V. Dua, Using Low-Grade Heat for Solvent Extraction based Efficient Water Desalination, Vol. 29 of Computer Aided Chemical Engineering, Elsevier, 2011. `doi:10.1016/B978-0-444-54298-4.50119-7`.

[34] J. Guo, Z. D. Tucker, Y. Wang, B. L. Ashfeld, T. Luo, Task-Specific Ionic Liquid Enables Highly Efficient Low Temperature Desalination by Directional Solvent Extraction, chemrxiv.org`doi:10.26434/chemrxiv.11840025.v1`.
URL `https://chemrxiv.org/articles/preprint/Task-Specific_Ionic_Liquid_Enables_Highly_Efficient_Low_Temperature_Desalination_by_Directional_Solvent_Extraction/11840025`

[35] S. A. Papoulias, I. E. Grossmann, A structural optimization approach in process synthesis -ii: Heat recovery networks, Computers & Chemical Engineering 7 (6) (1983) 707–721. `doi:10.1016/0098-1354(83)85023-6`.

[36] L. Biegler, I. Grossmann, A. Westerberg, Systematic methods for chemical process design, Prentice Hall, 1997.

[37] J. Bezanson, A. Edelman, S. Karpinski, V. B. Shah, Julia: A fresh approach to numerical computing, SIAM review 59 (1) (2017) 65–98.

[38] I. Dunning, J. Huchette, M. Lubin, JuMP: A modeling language for mathematical optimization, SIAM Review 59 (2) (2017) 295–320. `arXiv:1508.01982`, `doi:10.1137/15M1020575`.

[39] A. Wächter, L. T. Biegler, On the Implementation of a Primal-Dual Interior Point Filter Line Search Algorithm for Large-Scale Nonlinear Programming, Mathematical Programming 106 (1) (2007) 25–57.

[40] "HSL. A collection of Fortran codes for large scale scientific computation. http://www.hsl.rl.ac.uk/".

[41] M. B. Oliveira, M. J. Pratas, I. M. Marrucho, A. J. Queimada, J. A. P. Coutinho, Description of the mutual solubilities of fatty acids and water with the cpa eos, AIChE Journal 55 (6) (2009) 1604–1613. `doi:10.1002/aic.11766`.

[42] R. Battino, P. Seybold, Solubility correlations. part 1, Chemistry & Biodiversity 4 (11) (2007) 2547–2554. `doi:10.1002/cbdv.200790208`.

[43] NIST, National Institute of Standards and Technology[link].
URL `https://www.nist.gov`

[44] C. P. Fredlake, J. M. Crosthwaite, D. G. Hert, S. N. V. K. Aki, J. F. Brennecke, Thermophysical properties of imidazolium-based ionic liquids, Journal of Chemical & Engineering Data 49 (4) (2004) 954–964. `doi:10.1021/je034261a`.

[45] M. A. Duran, I. E. Grossmann, Simultaneous optimization and heat integration of chemical processes, AIChE Journal 32 (1) (1986) 123–138. `doi:10.1002/aic.690320114`.

[46] Year 2019 Industrial Firm Power Rates, Edison Electrical Institute.
URL `https://www.consultbai.com/images/stories/publications/maps20_388251.pdf`

[47] G. Ulrich, Chemical Engineering Process Design and Economics: A Practical Guide, Process Publishing, 2004.

[48] Foodchem International Corporation[link].
URL `https://foodchem.cn`

[49] A. Bardow, K. Steur, J. Gross, Continuous-molecular targeting for integrated solvent and process design, Industrial & Engineering Chemistry Research 49 (6) (2010) 2834–2840. `doi:10.1021/ie901281w`.

[50] Proionic[link].
URL `https://www.proionic.com/bestseller/EMIM-TFSI-electronic-grade.php`

[51] M. B. Shiflett (Ed.), Commercial Applications of Ionic Liquids, Springer, 2020.

[52] N. D. Austin, N. V. Sahinidis, D. W. Trahan, Computer-aided molecular design: An introduction and review of tools, applications, and solution techniques, Chemical Engineering Research and Design 116 (2016) 2–26, process Systems Engineering - A Celebration in Professor Roger Sargent's 90th Year. `doi:10.1016/j.cherd.2016.10.014`.

[53] R. Gani, Computer-aided methods and tools for chemical product design, Chemical Engineering Research and Design 82 (11) (2004) 1494 – 1504. `doi:10.1205/cerd.82.11.1494.52032`.

[54] L. Y. Ng, F. K. Chong, N. G. Chemmangattuvalappil, Challenges and opportunities in computer-aided molecular design, Computers & Chemical Engineering 81 (2015) 115 – 129. `doi:10.1016/j.compchemeng.2015.03.009`.

[55] E. A. Eugene, W. A. Phillip, A. W. Dowling, Data science-enabled molecular-to-systems engineering for sustainable water treatment, Current Opinion in Chemical Engineering 26 (2019) 122–130. `doi:10.1016/j.coche.2019.10.002`.

Supplementary information

Table 12: Stream results for reference design with decanoic acid as solvent using 50°C as maximum allowable temperature ΔT_{min}=6°C. See Figure 1 for schematics.

Stream	**Flow**	**Temperature**	x_d	x_w	x_s
	kmol/s	°C	%mol	%mol	%mol
1	0.5	25	0.00	98.89	1.11
2	0.5	50	0.00	98.89	1.11
3	5.16	50	69.79	30.18	0.03
4	0.25	50	10^{-3}	98.41	1.58
5	5.16	34	69.79	30.18	0.03
6	0.25	34	10^{-4}	99.37	0.62
7	4.91	34	73.33	26.66	10^{-4}
8	4.91	50	73.33	26.66	10^{-4}
9	5.16	50	66.56	33.33	0.10
10	0.25	25	10^{-3}	98.41	1.58
11	0.25	25	10^{-4}	99.37	0.63
12	10^{-4}	34	100	0.00	0.00
13	10^{-4}	50	100	0.00	0.00

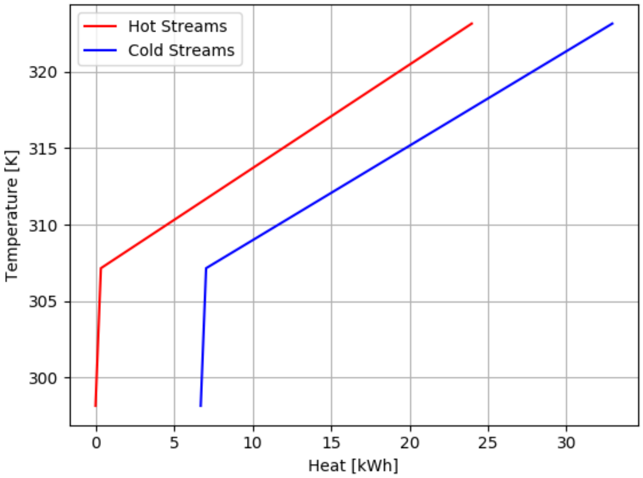

Figure 12: Composite curves for the reference design with decanoic acid as solvent using 50°C as maximum allowable temperature.